PARALLEL IMPLEMENTATION OF GALERKIN TECHNIQUE IN LARGE-SCALE ELECTROMAGNETIC PROBLEMS

Dimitra I. Kaklamani, Konstantina S. Nikita and Andy Marsh
Department of Electrical and Computer Engineering
Institute of Communication and Computer Systems
National Technical University of Athens
9 Iroon Polytechniou, Zografos 15780, Athens, Greece

ABSTRACT. An integral equation formulation in conjunction with a parallelised Galerkin technique is employed to solve large-scale electromagnetic (EM) problems. The proposed technique is applicable to EM structures consisting of similar conducting or dielectric parts, defined as "elements". Coupled integral equations are derived in the frequency domain, written in terms of the conductivity currents or the electric fields developed on the conducting or dielectric "elements" surfaces, respectively. The system of integral equations is numerically solved via the parallel computed Galerkin technique, with convenient entire domain basis functions. Even for electrically large structures, the use of entire domain basis functions leads to relatively small order linear systems and the main computational cost refers to the matrix fill rather than the matrix solution. The parallelisation introduced to the computation of the matrix elements overcomes the limitation of using Method of Moments at lower and resonant frequencies. The inherent parallelism of the introduced technique allows for the results to be obtained with minimal additional to the sequential code programming effort. Two indicative electromagnetic compatibility applications are presented, concerning the coupling of incident waves with multiple conducting rectangular plates and the coupling phenomena occurring in a multi-element waveguide array looking into a layered lossy cylinder. Numerical results are presented, while the applicability/suitability of diverse High Performance Computing platforms is judged, based on both performance obtained and ease of code portation.

Keywords: Method of Moments, Code Parallelisation, Electrically Large Structures.

1. INTRODUCTION

The analysis and design of complex realistic electromagnetic (EM) structures is limited by the relatively restricted computational power of the conventional sequential computers -even those of "main frame" or "vector processing" type- as well as by the vector nature of the EM radiation and the extended power radiation in the environment. The introduction of massively parallel computer architectures has opened new research horizons in this area (Davidson 1990). Indeed, the major advantage of applying High Performance Computing (HPC) to EM problems (Calalo et al. 1989, Davidson 1993, Fijany et al. 1995, Cwik et al. 1997, Lu et al. 1997) is the reduction of execution times of a given size of problem from days/hours to minutes/seconds, enabling the investigation of problems, that were so computationally expense, that they were practically "unsolvable". Pioneering research work in such areas becomes an arduous tedious endeavour. To fully exploit the computing power offered by available parallel platforms, the existing algorithms based on diverse numerical techniques must be re-examined with emphasis on their efficiency for parallel implementation.

Focusing on Method of Moments (MoM) algorithms (Harrington 1983), their use in solving large-scale EM problems is mainly restricted by the extensive computational cost in calculating the kernel elements and solving the resulting matrix equation. Aiming at reducing the storage requirements and speeding-up the solution algorithms on either von Neumann or parallel computers, a variety of basis functions, discretisation schemes and solvers have been employed (Davidson 1993, Aksun and Mittra 1993, Alanen 1991, Coen et al. 1994, Bornholdt and Medgyesi-Mitschang 1988). Subdomain, entire domain and mixed domain or hybrid Galerkin expansions have been used in the literature (Aksun and Mittra 1993, Alanen 1991, Coen et al. 1994, Bornholdt and Medgyesi-Mitschang 1988). Subdomain basis functions have been favored, due to their geometric flexibility and ability to handle localised surface features, apertures or feed-point distributions. Although the arising multiple integrals of the kernel matrix are relatively easily evaluated, the kernel matrix becomes of very large order for problems even slightly outside the resonance region, since at least ten basis functions are approximately required per wavelength. Therefore, when employing subdomain Galerkin technique, the main computational cost refers to the matrix solution and the choice of the proper discretisation scheme and solver is of major importance. Alternatively, smooth entire domain basis functions can be employed and, when successfully selected for a specific geometry, can lead to relatively small matrix dimensions even for electrically large structures. In this case, the main computational cost refers to the matrix fill and the efficient computation of its elements is very crucial.

In this context, a drastic reduction of the computation time is achieved in (Park and Ballanis 1997), by introducing an analytical technique to evaluate the asymptotic part of the kernel elements. Furthermore, taking advantage of the fact that any EM scattering solution can be analysed into high and low frequency components, a multilevel formulation of MoM has been presented in (Kalbasi and Demarest 1993), while in (Kaklamani and Marsh 1995), a parallel computed MoM technique is used to analyse fundamental electrically large planar conducting structures, both allowing substantial computational savings and therefore use of MoM to higher frequencies.

The present work also deals with the parallel implementation of Galerkin technique, providing an effective and accurate near-field solution to a system of frequency domain coupled integral equations modelling a class of canonical large-scale EM problems. Entire domain basis functions are used and emphasis is given on the efficient fill of the derived matrix. To this end, a parallel algorithm is developed, implementing a 12-point Gauss quadrature integration rule to compute the integrals of the kernel matrix, arising from the Galerkin technique procedure. In section 2, the parallelised Galerkin technique is presented and its applicability to different EM engineering areas is demonstrated. Two specific problems are solved, concerning the coupling of incident waves with multiple conducting rectangular plates and the coupling phenomena occurring in a multi-element waveguide array looking into a layered lossy cylinder. The former application also serves as a pilot problem, in order to demonstrate the inherent parallelism of the method that can be exploited. To this end, in section 3, different HPC platforms are utilised and their advantages are determined in terms of both performance obtained and ease of code portation. Finally, section 4 provides some concluding remarks.

2. PARALLEL COMPUTED ENTIRE DOMAIN GALERKIN TECHNIQUE

The technique presented in this section can be used to analyse a class of electrically large canonical structures consisting of similar dielectric or conducting parts, defined as "elements". In order to demonstrate its applicability, two specific electromagnetic compatibility (EMC) problems are treated.

The first problem deals with EM scattering from electrically large planar conductors. This is a subject of much research, since plates can be considered as building structures of more complex configurations (Alanen 1991, Peters and Volakis 1988, Kaklamani and Uzunuglu 1994, Ufimtsev 1996). Furthermore, employing Babinet's principle, the complementary problem of EM penetration through apertures "cut" on infinite planar conducting screens (Butler et al. 1978, Luebbers and Penney 1994) can also be considered, enlightening many EMC problems. The specific examined geometry is given in Fig. 1, where Q-number of perfectly conducting infinitesimal thickness rectangular plates, placed with identical orientation at arbitrary positions on planes parallel to the xy-plane, are presented.

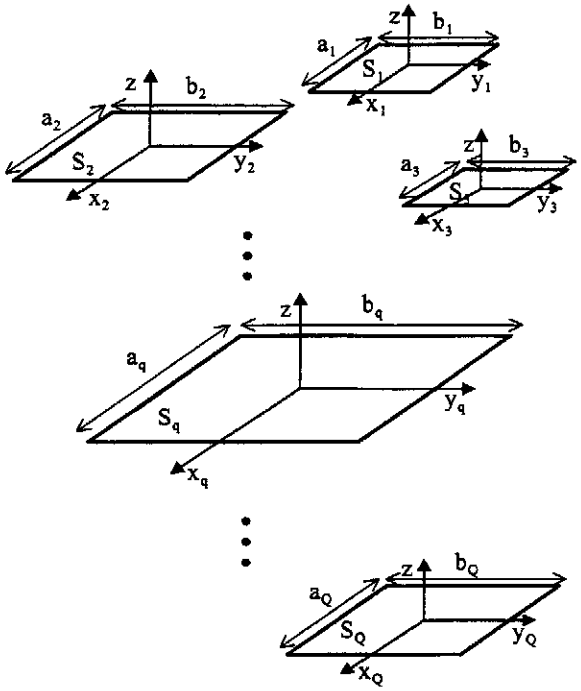

Fig. 1: Q-number of perfectly conducting infinitesimal thickness parallel rectangular plates.

The second problem deals with the analysis of coupling phenomena occurring in a concentric multi-waveguide array used to provide focusing inside a layered biological tissue model. Focusing of EM energy inside biological tissues is an important topic in many biomedical applications (Weiyian and Shoroung 1992, Arcangeli et al. 1984). For this purpose, until now, mainly the low microwave spectrum (100-1000 MHz) has been employed and continuous wave concepts have been applied, with limited success (Chen and Ghandhi 1992, Boag et al. 1993), while recently the use of a concentric multi-element waveguide array and pulsed signals of short pulse width with a high frequency (9.5 GHz) carrier has also been reported (Nikita and Uzunoglu 1996). However, in multi-element arrays significant interaction exists between system elements, resulting in non-predictable behaviour of this type of systems, as shown in (Nikita and Uzunuglu 1996) for concentric waveguide systems operating at low microwave frequencies. In the present paper, the investigation of coupling phenomena occurring in concentric waveguide arrays operating at higher frequencies is enabled by applying the parallelised Galerkin technique. The examined geometry consists of a three-layer cylindrical biological tissue model, irradiated by Q rectangular aperture waveguide applicators (Fig. 2).

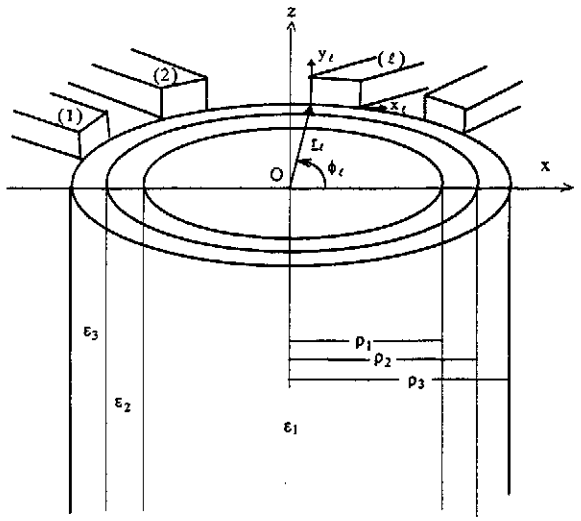

Fig. 2: Multi-waveguide array radiating into a three-layer biological tissue model.

In order to analyse the coupling of time harmonic EM fields with the structures shown in Figs. 1 and 2, a system of coupled integral equations is derived in terms of the unknown distribution on each "element" (conducting plate or waveguide aperture) surface, by using a Green's function approach or a phase space eigenwaves description approach. The operator form of the derived coupled system of integral equations is converted into a matrix equation by a Galerkin technique. Since structures of canonical shape are considered, entire domain basis functions are favored (see detailed formulations and analyses in (Kaklamani and Marsh 1995) and (Nikita and Uzunoglu 1996)). The order of the resulting kernel matrices depends upon the number of dielectric or conducting "elements" and mainly upon the frequency, increasing fast for problems even slightly outside the resonance region, since more basis functions are required to accurately describe the unknown tangential electric or magnetic field distribution on each "element" surface. It is important to emphasise that the "clever" choice of the entire domain basis functions results into relatively small order matrices and the main computational cost refers to the evaluation of the kernel matrix elements rather than the matrix solution. Working in the spectral domain, the arising integrals over the "elements" surfaces are analytically computed, while the infinite phase space integrals, associated to the Green's function Fourier transformation or to the eigenwave field description, are numerically evaluated, using a 12-point Gauss quadrature procedure (Abramowitz and Stegun 1970). The exact expressions of the arising integrals are given in the Appendix for both problems under investigation. Their computation constitutes the most time consuming part of the corresponding developed codes and is easily parallelised, by distributing the integration over 12 processors, without the need of inter-processor communication. If the integration path is divided into M independent Gauss calculations, it can be seen that, with minimal programming effort, the method has an inherent $12\times M$-fold parallelism. It is, therefore, envisaged that the computation times can be further reduced by a factor of M, if $12\times M$ processors are available. These characteristics allow for the algorithms to be ported to both shared and distributed memory machines without extensive programming effort. Nevertheless, since the contribution to the final value of the computed integrals is non-uniform along the integration path, special care has to be taken in distributing the corresponding calculations over the $12\times\ell$ processors, in order to avoid load imbalancing problems. A detailed examination of varying HPC platforms suitability is presented in section 3.

Indicative EM results obtained by applying the proposed parallel computed entire domain Galerkin technique are given in Figs. 3 and 4. The convergence and stability of the obtained solutions have been checked by increasing the number of basis functions used to describe the currents on the plates and the electric fields on the apertures. Considering the fact that the EM field expressions satisfy both the Maxwell's equations and the relevant boundary conditions, it is concluded that the derived results are self-consistent and accurate within the framework of the approximate solution of the system of coupled integral equations.

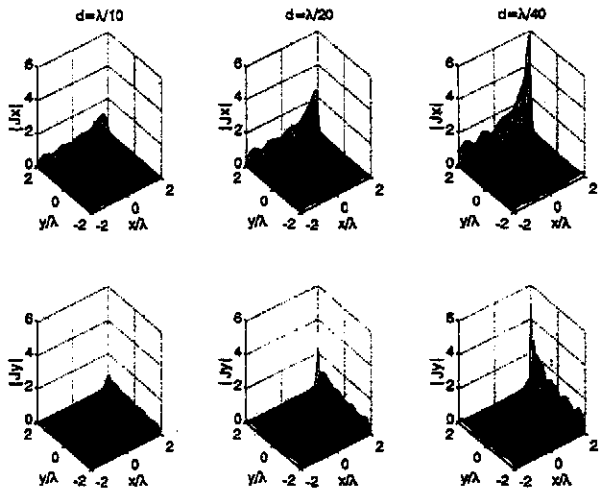

Fig. 3: Conductivity currents distribution induced on a $2\lambda\times2\lambda$ conducting plate lying in the xy-plane and excited by a y-oriented Hertzian dipole placed at a distance d above its right-back corner.

As far as the problem of EM scattering from electrically large conducting plates is concerned (see Fig. 1), the convergence rate of the conductivity currents induced precisely on the plates surfaces is the most important result concerning the accuracy of the proposed method, since it refers to near field quantities. Detailed convergence tests and comparison with published data concerning the single-plate problem are presented in (Kaklamani and Marsh 1995). Focusing on edge behaviour phenomena, in Fig. 3, it is shown how moving a y-oriented Hertzian dipole along the z

axis and towards the back-right corner of a $2\lambda \times 2\lambda$ rectangular plate, affects the conductivity currents distribution induced on the plate surface.

As far as the problem of a layered biological tissue model irradiated by a multi-waveguide array is concerned (see Fig. 2), the strength of coupling phenomena can be analysed, by exciting one element, and computing the TE_{10} mode coefficients coupled to the other elements (mutual coupling coefficients, S^c) and the coefficient of the reflected TE_{10} mode on the same aperture (self reflection coefficient, S^r). The parallelised Galerkin technique has been used to compute the coupling parameters in a 30-element TE_{10} waveguide (2×1 cm^2 aperture size) array placed symmetrically at the periphery of a cylindrical tissue model, 16 cm in diameter. The computations are carried out at the operation range ($1.1\,f_0$ - $1.8\,f_0$, f_0 being the cut-off frequency of the TE_{10} mode) of the system. The tissue model consists of two layers, simulating bone and brain tissues and it is surrounded by a 2 cm thick lossless dielectric layer. The thicknesses of the bone and the external dielectric layers are assumed to be $\rho_2 - \rho_1 = 0.5$ cm and $\rho_3 - \rho_2 = 2$ cm, respectively ($2\rho_3 = 20$ cm) (see Fig. 2). The dielectric constant of the external layer is taken to be $\varepsilon_3 = 2.1$. The numerical values of tissue complex permittivities used in the calculations are defined at the frequency range of interest by using the data compiled from the relevant literature (Gabriel et al. 1996). In Table 1, convergence patterns are presented at 9.5 GHz, in terms of the self reflection coefficient (S^r) and the mutual coupling coefficients with neighbouring (S^c_{ne}) and opposite (S^c_{op}) applicators, by increasing the number

Table 1. *Convergence of the self reflection coefficient S^r and mutual coupling coefficients (S^c_{ne}, S^c_{op}) for the configuration of Fig.2 at 9.5 GHz by increasing the number of aperture modes.*

Modes appearing on the excited aperture	S^r	S^c_{ne}	S^c_{op}
TE_{10}	0.61 $\angle$-14.35°	0.0091 $\angle$-44.9°	0.0027 $\angle$-126.6°
TE_{10} TE_{12} TM_{12}	0.612 $\angle$-15.2°	0.0123 $\angle$-41.7°	0.0024 $\angle$-130.3°
TE_{10} TE_{12} TE_{30} TE_{32} TM_{12} TM_{32}	0.6035 $\angle$-14.02°	0.011 $\angle$-42°	0.0025 $\angle$-128°

of modes appearing on the excited aperture. It can easily be observed that the subset of modes (TE_{10}, TE_{12}, TE_{30}, TE_{32}, TM_{12}, TM_{32}) appearing on applicator apertures is considered to be sufficient to assure convergence and accuracy. Numerical results for the strength of coupling between neighbouring (S^c_{ne}) and opposite (S^c_{op}) applicators in the examined 30-element waveguide array are presented in Fig. 4, at the operation range of the system. It is important to emphasise that in the obtained results, a detailed three-dimensional EM model is employed, which takes into account the modification of the field on each waveguide aperture resulted from the other radiating elements of the array, as well as from the presence of the lossy, layered, dielectric body standing at the near field region.

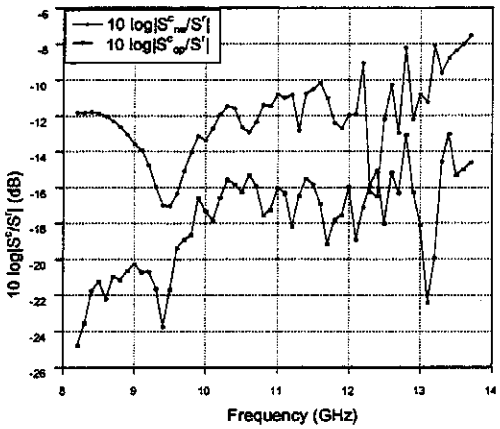

Fig. 4: *The ratio of the mutual coupling coefficient between neighbouring (S^c_{ne}) and opposite (S^c_{op}) applicators to the self reflection coefficient (S^r) in a symmetric configuration of 30 rectangular aperture (2×1 cm^2) waveguide applicators, placed at the periphery of a cylindrical body model of circular cross section, 20 cm in diameter, at the operation range of the system.*

3. IMPLEMENTATION ON VARIOUS HPC PLATFORMS

Due to the nature of the computation of the phase space integrals, which are the elements of the system kernel (see Appendix), the developed algorithm can be adapted for both shared-memory, distributed-memory and additionally vector processing HPC platforms. It has already been shown in (Kaklamani and Marsh 1995) that the code possesses a substantial amount of inherent parallelism, that can be exploited by a shared-memory architecture. Nevertheless, varying HPC platforms can exploit the different degrees of parallelism inherent in the algorithm.

The first application, shown in Fig.1, concerning the EM illumination of Q number of conducting rectangular plates lying on parallel planes, also serves as a pilot problem, in order to answer the emerging question, which HPC platform to use in solving more complex EM problems. For reasons of CPU time savings, the case Q=1 and a_1=b_1 (i.e. one square plate) is chosen for the benchmarking process. Small, intermediate and large size problems (N=8, N=98 and N=512 respectively, with N denoting the order of the derived linear system) are solved on each HPC plat-

form and the corresponding CPU times are compared. There are two crucial points that should be noted here. Firstly, the three orders of systems that have been selected (N=8, N=98, N=512) are only indicative, in order to demonstrate the scalability of the proposed method. That is, by filling and solving the same order system, other geometries (e.g. larger number of plates at a lower frequency) can be solved. Secondly, the characterisation of the three cases as small, intermediate and large size problems is not referred to the absolute value of the system order, but to the electrical size of the problem that can be treated. The system order is in any case small, due to the employment of entire domain basis functions. For example, by the N=512 system, the case of one square plate of 10λ side can be accurately solved.

The HPC platforms currently evaluated are the Silicon Graphics Power Challenge and Intel Paragon, both located at the NTUA, Greece and the CRAY C90 and CRAY T3D, both located at CINECA, Italy. The shared-memory Silicon Graphics Power Challenge has 14 TFP Processors (MIPS R8000 CPU & MIPS R8010 FPU), a 16K data cache, a 16K instruction cache and 8-way interleaved main memory of 1024 Mbytes, providing a peak performance of 4.2 Gflops, while the distributed-memory Intel Paragon XP/S has 48 processing nodes with i860 processors, providing a peak performance of 48 × 75 Mflops = 3.6 Gflops. The shared-memory CRAY vector processing C-90 has 2 × 1 Gflops vector processing CPU's providing a peak performance of 2 Gflops and the massively parallel distributed-memory CRAY T3D has 64 processing nodes providing a peak performance of 64 × 150 Mflops = 9.6 Gflops. Each of the HPC platforms is judged on both performance obtained and ease of code portation, which is directly related to the extent of extra needed code.

Before comparing these four computing platforms, some generalised assumptions need to be mad. Firstly, the platforms are aimed to be used only as computational tools. The main concern is related to the ease of code portation and the ability to solve the largest problem in a given tolerable period of time, without getting involved with the pragmatics and detailed code optimisations. Secondly, if a computational platform with a performance of 1 Gflop takes τ hours to solve a given problem, then the same platform with a 2 Gflops performance would need $\tau/2$ hours to solve the same problem. Thirdly, since the platforms are of different sizes and costs, two performance figures are of interest: the absolute time taken to solve a given problem ("absolute performance") and an estimated relative time taken to solve the same problem ("relative performance"). This relative time is calculated as the time taken if the platform had a 1 Gflop peak performance. These assumptions enable trans-architectural platforms to be composed at an abstract level, without getting involved with complex benchmarks etc., as discussed in detail in the following and summarised in Table 2.

As far as the shared-memory SGI Power Challenge platform is concerned, the 12-point quadrature Gauss algorithm is parallelised, by subdividing the integration path and splitting the corresponding calculations onto 12 processors. This is achieved, by the hand addition of a single line of code, containing the parallel directive C$DOACROSS. For brevity and ease of porting the code, only 12 of the possible 14 TFP processors are used. The peak performance used is therefore 12 × 300 Mflops = 3.6 Gflops. The consumed CPU time is 40 seconds for N=8, 23 minutes for N=98 and approximately 25 hours for N=512, resulting in relative performances of approximately 3.6 × 40 = 144 seconds, 3.6 × 1380 = 4968 seconds and 3.6 × 9000 = 32400 seconds respectively (see Table 2). The large size problem CPU time (25 hours) also includes a large overhead, due to page swapping, incurred by accessing huge data arrays. Fortunately, the porting from standard FORTRAN 77 to the SGI Power FORTRAN has only taken 30 minutes of programming and consultation effort. When employing more rigorous optimisation techniques, such as using the full potential of software pipelining and the SGI PFA (Parallel FORTRAN Accelerator), it is probable that these execution times will be considerably further reduced.

Table 2. *Performance comparison of diverse HPC machines.*

Machine		SGI Power Challenge	Intel Paragon XP/S	CRAY C-90	CRAY T3D
Peak Performance (Gflops)		3.6	2775	2.0	9.0
Absolute Perform. (sec)	N=8	40	47	255	26
	N=98	1380	2940	1960	2040
	N=512	9000	16920	12240	-
Relative Perform. (sec)	N=8	144	130	510	234
	N=98	4968	8158	3920	18360
	N=512	32400	46953	24480	-

Due to the fact that the algorithm can be divided to M independent Gauss calculations, as described in section 2, a greater number of processors can be used. Therefore, the parallelisation of the algorithm or the distributed-memory Intel Paragon XP/S consists in using 37, out of the possible 48, i860 processing nodes; 3 groups of 12 slave processing nodes (i.e. M=3 independent Gauss calculations) and a master controlling processing node, leading to a peak performance of 37 × 75 Mflops = 2.775 Gflops. Communication between processing nodes is accomplished via explicit message-passing. Each group of 12 processing nodes concentrates on the parallelisation of a single 12-point quadrature Gauss algorithm,

analogous to the SGI approach. It was seen, however, that this resulted in load imbalances, because of the fact that all the kernel integrands given by eq. (A.1) vary more rapidly with the increase of k; therefore, when integrating with respect to the φ_k-variable more subdivisions must be considered for large k values, leading to further computational cost with the k increase. After an explicit investigation, the optimum distribution was derived. To this end, the porting from standard FORTRAN 77 to the Paragon platform has taken about 2 hours involving about 15 modifications of the original code. These modifications involve the introduction of the message-passing constructs *irecv* and *isend* and the explicit subdivision of the total computation over the 36 slave processing elements. The consumed CPU time is 47 seconds for N=8, 49 minutes for N=98 and approximately 47 hours for N=512, resulting in relative performances of $2.775 \times 47 \approx 130$ seconds, $2.775 \times 2940 \approx 8158$ seconds and $2.775 \times 16920 = 46953$ seconds respectively (see Table 2). As it is expected, due to the peak performances offered, the Paragon performs slower than the SGI machine. However, what is more disappointing is the relative performances of the Paragon compared to the SGI machine. For example, when N=98, the relative performance of the Paragon machine is 81158 seconds compared with the SGI machine relative performance of 4968 seconds. In this case, for this example, a Paragon machine with 1.6 times the peak performance of the SGI machine would be required to solve the given problem in the same time. Clearly some work has to be done to optimise the data locality, when using the Paragon to solve problems with very large data arrays. It must be noted that, when N=98, the message-passing and system overheads represents about 2% of the total execution time, whereas, when N=512, this value increases to 25%. From these initial investigations, it can be seen that, the algorithm possesses an inherent coarse-grained parallelism that can be exploited by both architectural models.

The suitability of the CRAY C-90 architecture is also investigated, to see if the algorithm possesses a substantial fine-grain parallelism, that could be exploited by a vector processor. Each of the two CPUs of the CRAY C-90 is a vector processor with 128 banks, a clock of 4 ns and a memory speed of 88 ns. The exploitation of vectorisation and parallelisation is achieved by the CRAY cf77 compiler with default settings and with aggressive optimisation switched on. The addition of two vector processing directives (CDIR$ IVDEP) leads to further reduction of the execution times. The porting process required about 1 hour. It consisted mainly in examining the code listing for further vectorisable loops and introducing 2 line modifications. The consumed CPU time is 255 seconds for N=8, 33 minutes for N=98 and approximately 34 hours for N=512, resulting in relative performances of $2.0 \times 255 = 510$ seconds, $2.0 \times 1960 = 3920$ seconds and $2.0 \times 12240 = 24480$ seconds respectively (see Table 2). This indicates that the algorithm contains a significant amount of fine-grain parallelism that can be exploited by the vector processor. The relative performances are impressive, out performing the SGI platform. For example, from the relative performances for N=98, it can be seen that the CRAY C-90 with 2.0×1 Gflop = 2 Gflops peak performance would be equivalent to a SGI with $4968/(3920/2.0) = 2.53$ Gflops peak performance (9×300 Mflops processors). Considering the ease of portability and absolute performance of the CRAY C-90, it remains a realistic alternative shared-memory platform. However, both CRAY C-90 and SGI platforms have the memory access bottleneck, when considering larger problem sizes.

An alternative to the Intel Paragon distributed-memory platform is the CRAY T3D, a superscalar architecture with 64 processing nodes. Each node is based on the DEC α 21064 chip providing a peak performance of 150 Mflops, with a clock of 6.67ns. The limiting factor, however, is the 8 Kbytes data cache and the 8 Kbytes instruction cache. Although possessing facilities for PVM and message-passing, the work sharing on shared data paradigm was used. To this end, porting from standard FORTRAN 77 to the MPP FORTRAN has required about 30 minutes programming effort, involving definition of a global (shared) array to collect the results and explicit subdivision of the computation, similar to the Paragon approach. For brevity, 60 processing nodes are used, providing a peak performance of 60×150 Mflops = 9.0 Gflops, divided in 5 groups of 12 processing nodes. Each group of processing nodes is responsible for a Gauss calculation, similar to that implemented on the Paragon. Due to load balancing, one group of processors performs two Gauss calculations. The resulting performance is only 26 seconds for N=8 and 34 minutes for N=98, while the estimated performance for N=512 is 10 hours (see Table 2). The CRAY T3D could be used for benchmarking purposes only for up to 8 hours. Therefore, there are no available results for the absolute performance in solving the N=512 problem and the estimated performance of 10 hours is considered to be adequate for the current research. It must be noted that, these results are achieved without any optimisation and there exists a load imbalance. Taking these factors into consideration, the performances are impressive.

It can be concluded that, for both ease of portation and resulting performance the shared-memory Silicon Graphics (and to a lesser extent the CRAY C-90) and the distributed-memory CRAY T3D appear to be more suitable in solving problems in the domain of electrically large EM structures. However, the potential of the shared-memory platforms for solving even larger problem sizes is limited by the memory access, whereas the distributed-memory model is modularly extendible and, in the authors' opinion, more suitable in solving even larger problem sizes. It must also be noted that the work sharing paradigm adopted by the

CRAY T3D provides an appealing alternative to message-passing approaches, making programming large distributed-memory machines, to solve large problem sizes, a realistic possibility.

4. CONCLUSIONS

HPC has been employed in order to extent MoM for the treatment of a certain class of large-scale EM problems. Namely, a parallel computed Galerkin technique in conjunction with a frequency-domain coupled integral equation formulation has been adopted, applicable to electrically large structures consisted of similar conducting or dielectric parts.

The resulting algorithm parallelisation overcame the limitation of using MoM at lower and resonant frequencies, while the inherent parallelism of the introduced technique allowed for the results to be obtained with minimal additional to the sequential code programming effort. Namely, the phase space integrals, appearing in the system kernel have been computed numerically employing a 12-point quadrature Gauss algorithm, which has been parallelised, by subdividing the integration path and splitting the corresponding calculations over various HPC platforms. For both ease of portation and resulting performance the shared-memory Silicon Graphics and the distributed-memory CRAY T3D appear to be more suitable, though the potential of the shared-memory platforms for solving even larger problem sizes is limited by the memory access, whereas the distributed-memory model is modularly extendible and, therefore, more suitable in solving even larger problem sizes.

Two specific EMC applications were solved, concerning the coupling of incident waves with multiple conducting rectangular plates and the coupling phenomena occurring in a multi-element waveguide array looking into a layered lossy cylinder, while numerical results were computed for indicative cases. Due to the algorithm parallelisation, the computation times became tolerable, allowing the problems' size, hence the accuracy, to be increased. The convergence rate of near-field quantities excited on electrically large structures is the most important result concerning the accuracy of the proposed method, while following the same approach, more complex configurations can be constructed and analysed.

5. APPENDIX

In solving the Q number of conducting rectangular plates structure shown in Fig. 1, the analytical expressions of the system kernel sub-matrices are defined as

$$\underline{\overline{K}}^{\ell q}_{nmn'm'} = \frac{\omega\mu_0}{8\pi k_0^2}\iint_{\Omega_k} d\underline{\tilde{k}}\left(\frac{e^{-j[q_0\,\mathrm{sgn}(z_\ell^0-z_q^0)(z_\ell^0-z_q^0+\delta_\ell)]}}{q_0}\right.$$
$$\left.\times\frac{e^{-j[q_0\,\mathrm{sgn}(-k_x(x_\ell^0-x_q^0)-k_y(y_\ell^0-y_q^0))}}{q_0}\right.$$
$$\left.\times\underline{\overline{U}}_{\ell_{n'm'}}(-\underline{\tilde{k}})\cdot\underline{\overline{A}}(\underline{\tilde{k}})\cdot\underline{\overline{U}}_{q_{nm}}(\underline{\tilde{k}})\right), \qquad (A.1)$$

where (q=1,2,...,Q ; ℓ=1,2,...,Q),

$$\iint_{\Omega_k} d\underline{\tilde{k}} \equiv \int_{-\infty}^{+\infty} dk_x \int_{-\infty}^{+\infty} dk_y \equiv \int_0^{+\infty} dkk \int_0^{2\pi} d\varphi_k\,,$$

$$\underline{\tilde{k}} = k_x\hat{x} + k_y\hat{y} = k(\cos\varphi_k\hat{x} + \sin\varphi_k\hat{y})\,, \qquad (A.2)$$

$k_0 = \omega\sqrt{\varepsilon_0\mu_0}$ is the free space propagation constant, ω is the angular frequency, ε_0 and μ_0 are the free space dielectric permittivity and magnetic permeability respectively, $\underline{r}_q^0 = x_q^0\hat{x} + y_q^0\hat{y} + z_q^0\hat{z}$ denotes the position vector of the q-th plate centre of gravity with respect to a global system of coordinates (x,y,z), $\delta_\ell \to 0^+$,

$$q_0 = q_0(\underline{\tilde{k}}) = \sqrt{k_0^2 - k^2}$$
$$\text{with } \mathrm{Re}(q_0)>0 \;\&\; \mathrm{Im}(q_0)<0, \qquad (A.3)$$

as required by the $\exp(j\omega t)$ time dependence and the satisfaction of the radiation condition at infinity,

$$\underline{\overline{A}}(\underline{\tilde{k}}) = \underline{\overline{A}}(k,\varphi_k) = (k_0^2 - k_x^2)\hat{x}\hat{x} - k_xk_y(\hat{x}\hat{y} + \hat{y}\hat{x}) + (k_0^2 - k_y^2)\hat{y}\hat{y}\,, \qquad (A.4)$$

and

$$\underline{\overline{U}}_{q_{nm}}(\underline{\tilde{k}}) = \frac{(n+1)J_{n+1}(-\frac{k_xa_q}{2})J_m(-\frac{k_yb_q}{2})}{2j^{(n+m)}k_x/(b_q\pi^2)}\hat{x}\hat{x} + \frac{(m+1)J_{m+1}(-\frac{k_yb_q}{2})J_n(-\frac{k_xa_q}{2})}{2j^{(n+m)}k_y/(a_q\pi^2)}\hat{y}\hat{y}\,, \qquad (A.5)$$

with $J_\nu(x)$ denoting the Bessel function of the first kind of ν-th order and $S_q = a_q \times b_q$, (q=1,2,...,Q) denoting the finite zero-thickness q-th conducting plate surface. The kernel elements encountered in the problem of Fig. 2 are of the following type:

$$K_{pn}^{\ell q} = \iint_{S_t} dxdy \iint_{S_q} dx'dy' \underline{h}_{p,t}(x,y)\cdot\underline{\overline{K}}_{tq}(x,y/x',y')\cdot\underline{e}_{n,t}(x',y')$$

where S_ℓ is the aperture of the $\ell-$th waveguide, $\underline{e}_{n,t}$ and $\underline{h}_{n,t}$ are the transverse electric and magnetic

fields of the waveguide normal modes, respectively, being of TE or TM type and

$$\overline{\underline{K}}_{\ell q}(x,y/x',y') = \int_{-\infty}^{+\infty} dk \sum_{m=-\infty}^{+\infty} \left(e^{jm(\phi_\ell-\phi_q)} e^{jm\left(-\frac{x}{\rho_3}+\frac{x'}{\rho_3}\right)}\right) \times e^{jk(y-y')}\overline{\underline{N}}(m,k) - \delta_{\ell q}\,\overline{\underline{\Omega}}(x,y/x',y')\Big), \qquad \text{(A.6)}$$

In eq. (A.6), $(\ell = 1,2,...,Q; q = 1,2,...,Q)$, $\delta_{\ell q}$ is the Kronecker's delta,

$$\overline{\underline{N}}(m,k) = \frac{1}{(2\pi)^2}\frac{jk_3}{\omega\mu_0\mu_3\rho_3}\overline{\underline{L}}'(m,k;\rho_3)\left(\overline{\underline{L}}(m,k;\rho_3)\right)^{-1}$$

$$\overline{\underline{\Omega}}(x,y/x',y') = \sum_{n=1}^{\infty}\left\{\left(-\frac{\gamma_n}{\omega\mu_0}\right)\underline{h}_{n,t}^{TE}\,\underline{e}_{n,t}^{TE} + \left(\frac{\omega\varepsilon_0}{\lambda_n}\right)\underline{h}_{n,t}^{TM}\,\underline{e}_{n,t}^{TM}\right\}, \qquad \text{(A.7)}$$

with γ_n, λ_n being the propagation constants of the TE and TM modal fields, respectively and $k_3 = k_0\sqrt{\varepsilon_3}$. The matrices involved in (A.7) are given by the following equations:

$$\overline{\underline{L}}'(m,k;\rho_3) = \overline{\underline{T}}_{3m}^{(1)}(k;\rho_3) + \frac{Z_m^{(2)}(\alpha_3\rho_3)}{Z_m^{(1)}(\alpha_3\rho_3)}\overline{\underline{T}}_{3m}^{(2)}(k;\rho_3)\overline{\underline{R}}_{3m},$$

$$\overline{\underline{L}}(m,k;\rho) = \overline{\underline{D}}_{3m}^{(1)} + \frac{Z_m^{(2)}(\alpha_3\rho)}{Z_m^{(1)}(\alpha_3\rho)}\overline{\underline{D}}_{3m}^{(2)}\overline{\underline{R}}_{3m}$$

where

$$\overline{\underline{D}}_{im}^{(q)}(k;\rho) = \begin{pmatrix} -\dfrac{\partial Z_m^{(q)}(\alpha_i\rho)/\partial\rho}{Z_m^{(q)}(\alpha_i\rho)} & -\dfrac{mk}{k_i\rho} \\ 0 & \dfrac{\alpha_i^2}{k_i} \end{pmatrix},$$

$$i = 3/q = 1,2 \qquad \text{(A.8)}$$

$$\overline{\underline{T}}_{im}^{(q)}(k;\rho) = \begin{pmatrix} -\dfrac{mk}{k_i\rho} & -\dfrac{\partial Z_m^{(q)}(\alpha_i\rho)/\partial\rho}{Z_m^{(q)}(\alpha_i\rho)} \\ \dfrac{\alpha_i^2}{k_i} & 0 \end{pmatrix},$$

$$i = 3/q = 1,2 \qquad \text{(A.9)}$$

with $Z_m^{(1)}(\alpha_i\rho) = J_m(\alpha_i\rho)$ and $Z_m^{(2)}(\alpha_i\rho) = Y_m(\alpha_i\rho)$, $k_i = k_0\sqrt{\varepsilon_i}$, $\alpha_i = \left(k_i^2 - k^2\right)^{1/2}$,

$$\overline{\underline{R}}_{3m} = \frac{Z_m^{(1)}(\alpha_3\rho)}{Z_m^{(2)}(\alpha_3\rho)}\left(\overline{\underline{T}}_{3m}^{(2)} - \frac{k_2}{k_3}\overline{\underline{G}}_{2m}\overline{\underline{F}}_{2m}\overline{\underline{D}}_{3m}^{(2)}\right)^{-1} \times\left(-\overline{\underline{T}}_{3m}^{(1)} + \frac{k_2}{k_3}\overline{\underline{G}}_{2m}\overline{\underline{F}}_{2m}\overline{\underline{D}}_{3m}^{(1)}\right) \text{ at } \rho = \rho_2 \qquad \text{(A.10)}$$

The matrices involved in (A.10) are

$$\overline{\underline{G}}_{2m}(k;\rho) = \overline{\underline{T}}_{2m}^{(1)} + \frac{Z_m^{(2)}(\alpha_2\rho)}{Z_m^{(1)}(\alpha_2\rho)}\overline{\underline{T}}_{2m}^{(2)}\overline{\underline{R}}_{2m},$$

$$\overline{\underline{F}}_{2m}(k;\rho) = \left[\overline{\underline{D}}_{2m}^{(1)} + \frac{Z_m^{(2)}(\alpha_2\rho)}{Z_m^{(1)}(\alpha_2\rho)}\overline{\underline{D}}_{2m}^{(2)}\overline{\underline{R}}_{2m}\right]^{-1},$$

$$\overline{\underline{R}}_{2m} = \frac{Z_m^{(1)}(\alpha_2\rho)}{Z_m^{(2)}(\alpha_2\rho)}\left(\overline{\underline{T}}_{2m}^{(2)} - \frac{k_1}{k_2}\overline{\underline{T}}_{1m}^{(1)}(\overline{\underline{D}}_{1m}^{(1)})^{-1}\overline{\underline{D}}_{2m}^{(2)}\right)^{-1} \times\left(\frac{k_1}{k_2}\overline{\underline{T}}_{1m}^{(1)}(\overline{\underline{D}}_{1m}^{(1)})^{-1}\overline{\underline{D}}_{2m}^{(1)} - \overline{\underline{T}}_{2m}^{(1)}\right) \text{ at } \rho = \rho_1 \qquad \text{(A.11)}$$

The matrices $\overline{\underline{D}}_{im}^{(q)}$, $\overline{\underline{T}}_{im}^{(q)}$, $i = 1,2$ and $q = 1,2$, appearing in (A.11), are obtained from eq. (A.8) and eq. (A.9), respectively, for i=1,2.

6. REFERENCES

Abramowitz M. and I.A. Stegun, ***Handbook of Mathematical Functions***, Dover Publications, Inc., New York, 875-924, (1970).

Aksun M.I. and R. Mittra, "Choices of Expansion and Testing Functions for the Method of Moments Applied to a Class of Electromagnetic Problems", ***IEEE Trans. Microwave Theory Tech.***, MTT-41, 503-509, (1993).

Alanen E., "Pyramidal and Entire Domain Basis Functions in the Method of Moments", ***J. Electro. Waves Applic.***, 5, 315-329, (1991).

Arcangeli G., P.P. Lombardini, G.A. Lovisolo, G. Marsiglia and M. Piatelli, "Focusing of 915 MHz Electromagnetic Power on Deep Human Tissues", ***IEEE Trans. Biomed. Eng.***, BME-31, 47-52, (1984).

Boag A., Y. Leviatan and A. Boag, "Analysis and Optimization of Waveguide Multiapplicator Hyperthermia Systems", ***IEEE Trans. Biomed. Eng.***, BME-40, 946-952, (1993).

Bornholdt J.M. and L.M. Medgyesi-Mitschang, "Mixed-Domain Galerkin Expansions in Scattering Problems", ***IEEE Trans. Antennas Propag.***, AP-36, 216-227, (1988).

Butler C.M., Y. Rahmat-Samii and R. Mittra, "Electromagnetic Penetration through Apertures in Conducting Surfaces", ***IEEE Trans. Antennas Propag.***, AP-26, 82-93, (1978).

Calalo R.H., T.A. Cwik, W.A. Imbriale, N. Jacobi, P.C. Liewer, T.G. Lockhart, G.A. Lyzenga and J.E. Patterson, "Hypercube Parallel Architecture Applied to Scattering Electromagnetic Problems", ***IEEE Trans. Magnetics,*** 24, 4, 2888-2890, (1989).

Chen J. and O.P. Ghandhi, "Numerical Simulation of Annular Phased Arrays of Dipoles for Hyperthermia of Deep Seated Tumors", ***IEEE Trans. Biomed. Eng.***, BME-39, 209-216, (1992).

Coen G., N. Fache and D. De Zutter, "Comparison Between Two Sets of Basis Functions for the Current Modeling in the Galerkin Spectral Domain Solution for Microstrips", ***IEEE Trans. Microwave Theory Tech.***, MTT-42, 505-513, (1994).

Cwik T., D.S. Katz and J. Patterson, "Scalable Solutions to Integral Equation and Finite Element Simulations", ***IEEE Trans. Antennas Propag.***, AP-45, 544-555, (1997).

Davidson D.B., "Parallel Matrix Solvers for Moment Method Codes for MIMD Computers", ***ACES Journal***, 8, 2, 144-175, (1993).

Davidson, D.B., "A Parallel Processing Tutorial", ***IEEE Antennas and Propagation Mag.***, 32, 2, 6-19, (Apr. 1990).

Fijany A., M.A. Jensen, Y. Rahmat-Samii and J. Barhen, "A Massively Parallel Computation Strategy for FDTD: Time and Space Parallelism Applied to Electromagnetics Problems", ***IEEE Trans. Antennas Propag.***, AP-43, 1441-1449, (1995).

Gabriel C., S. Gabriel and E. Corthout, "The Dielectric Properties of Biological Tissues", ***Med. Phys.***, 41, 2231-2293, (1996).

Harrington R.F., ***Field Computation by Moment Methods***, New York: Macmillan, Florida: Krieger Publishing, (1983).

Kaklamani D.I. and A. Marsh, "Solution of Electrically Large Planar Scattering Problems Using Parallel Computed Method of Moments Technique", ***J. Electro. Waves Applic.***, 9, 10, 1313-1337, (1995).

Kaklamani D.I. and N.K. Uzunoglu, "Scattering from a Conductive Rectangular Plate Covered by a Thick Dielectric Layer and Excited from a Dipole or a Plane Wave", ***IEEE Trans. Antennas Propag.***, AP-42, 1065-1076, (1994).

Kalbasi K. and K.R. Demarest, "A Multilevel Formulation of the Method of Moments", ***IEEE Trans. Antennas Propag.***, AP-41, 589-599, (1993).

Lu Y., and C.Y. Shen, "A Domain Decomposition Finite Difference Method for Parallel Numerical Implementation of Time-Dependent Maxwell's Equations", ***IEEE Trans. Antennas Propag.***, AP-45, 556-562, (1997).

Luebbers R. and C. Penney, "Scattering from Apertures in Infinite Ground Planes Using FDTD", ***IEEE Trans. Antennas Propag.***, AP-42, 731-736, (1994).

Nikita K.S. and N.K. Uzunoglu, "Analysis of Focusing of Pulse Modulated Microwave Signals Inside a Tissue Medium", ***IEEE Trans. Microwave Theory Tech.***, MTT-44, 1788-1798, (1996).

Nikita K.S. and N.K. Uzunoglu, "Coupling Phenomena in Concentric Multi-Applicator Phased Array Hyperthermia Systems", ***IEEE Trans. Microwave Theory Tech.***, MTT-44, 65-74, (1996).

Park S.-O. and C.A. Balanis, "Analytical Technique to Evaluate the Asymptotic Part of the Impedance Matrix of Sommerfeld-Type Integrals", ***IEEE Trans. Antennas Propag.***, AP-45, 798-805, (1997).

Peters T.J. and J.L. Volakis, "Application of the Conjugate Gradient FFT Method to Scattering from Thin Planar Material Plates", ***IEEE Trans. Antennas Propag.***, AP-36, 518-526, (1988).

Ufimtsev P.Y., "Comments on Diffraction Principles and Limitations of RCS Reduction Techniques", ***Proc. IEEE,*** 84, 1830-1851, (1996).

Weiyian W. and Z. Shoroung, "Unrelated Illumination Method for Electromagnetic Inverse Scattering of Inhomogeneous Lossy Dielectric Bodies", ***IEEE Trans. Antennas Propag.***, AP-40, 1292-1296, (1992).